Pegylated Phospholipid Micelles Induce Endoplasmic Reticulum-Dependent Apoptosis of Cancer Cells but not Normal Cells

Jing Wang,[†,‡,§] Xiaocui Fang,[†,‡,§] and Wei Liang[†,*]

[†]Protein and Peptide Pharmaceutical Laboratory, National Laboratory of Biomacromolecules, Institute of Biophysics, Chinese Academy of Sciences, Beijing, China, and [‡]Graduate School of Chinese Academy of Sciences, Beijing, China. [§]J.W. and X.F. contributed equally to this work.

ABSTRACT The rapid developments in nanotechnology have brought with them a deep concern over the safety of nanomaterials. Investigating the molecular mechanisms underlying their toxicity in different cell lines will help us better understand and apply nanomaterials appropriately. Poly(ethylene glycol)—phosphoethanolamine (PEG—PE) is an FDA-approved nonionic diblock copolymer and is widely used in drug delivery systems. Here, we find that PEG—PE accumulates in the endoplasmic reticulum (ER) and induces ER stress and that cancer cells and normal cells have different cell fates as a result of this stress. In A549 cancer cells, PEG—PE damages ER functions and triggers apoptosis by activating proapoptotic UPR signaling and high expression of cell death effector CHOP and proapoptotic Bax/Bak. In addition, PEG—PE-induced ER stress also up-regulates lipid synthesis and triggers lipid droplet formation in cancer cells. By contrast, in MRC-5 and 293T cells, high expression of the UPR feedback protein GADD34 which inhibits proapoptotic UPR signaling, and antiapoptotic Bcl-2 and Bcl-xl which down-regulate Bax/Bak, protect these normal cells from PEG—PE-induced apoptosis. When *gadd34*, *bcl-2*, or *bcl-xl* is knocked down, apoptosis occurs in PEG—PE-treated normal cells. In summary, we demonstrate the safety of PEG—PE in normal cells and elaborate the molecular mechanism underlying its nanotoxicity in cancer cells. This study implies PEG—PE-based drug delivery system has the potential to alter the sensitivity of cancer cells to some chemotherapeutic agents by selectively activating unfolded protein response (UPR) in cancer cells, and it also provides a useful foundation for research on ER stress-induced nanotoxicity and other lipid-based nanomaterials.

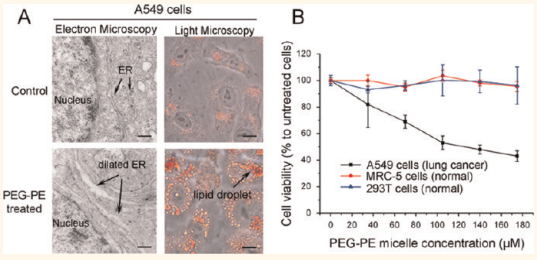

KEYWORDS: micelles · biocompatibility · ER stress · unfolded protein response · Bcl-2 family protein · apoptosis

Rapid developments in nanotechnology have brought with them a deep concern over the safety of nanomaterials.[1] Many reports indicate that inorganic nanomaterials induce different levels of cytotoxicity.[2] TiO_2 and SiO_2 nanoparticles accumulate in the nucleus and cause genotoxicity *via* direct interactions with DNA molecules and/or nucleoproteins.[3] Fullerenes and carbon nanotubes accumulate in the mitochondria and disrupt the mitochondrial electron transduction chain, generating oxidative stress and inducing apoptosis.[4] Toxicity induced by organic nanomaterials is less reported. Cationic dendrimers and lipids can disrupt cell membranes *via* nanohole formation and membrane erosion due to their interactions with negatively charged biological membranes.[5] However, many polymers are biodegradable or inert and have little or no toxicity to animals and humans.[6,7] They can be developed as drug delivery carriers and repair materials because of their safety and benefits in pharmaceutics and biology.[8] Poly(ethylene glycol)—phosphoethanolamine (PEG—PE) is one of the most promising polymers used as a carrier for anticancer drug delivery.[9]

PEG—PE, a diblock copolymer, consists of hydrophobic PE and hydrophilic PEG and spontaneously aggregates to form nanoscale micelles in water. In a previous study, we demonstrated that PEG—PE molecules can insert into cell membranes without disrupting membrane integrity and that these PEG—PE molecules are then transported into cells through nonspecific endocytosis and finally accumulate in the endoplasmic reticulum (ER).[10] The ER is an organelle that plays an essential role in multiple cellular processes required for cell survival and function, including intracellular calcium homeostasis, protein secretion, and lipid biosynthesis.[11] Previous studies showed that the excessive accumulation of cholesterol or saturated fatty acids in the ER can induce ER stress and activate the unfolded protein response (UPR).[12,13] We hypothesize that similar cellular events may occur in PEG—PE-treated cells since PEG—PE has a tendency to accumulate in the ER. To test this hypothesis, we investigated the molecular events related to ER stress and UPR activation in cancer cells

* Address correspondence to weixx@sun5.ibp.ac.cn.

Received for review February 8, 2012 and accepted May 6, 2012.

Published online May 06, 2012
10.1021/nn300571c

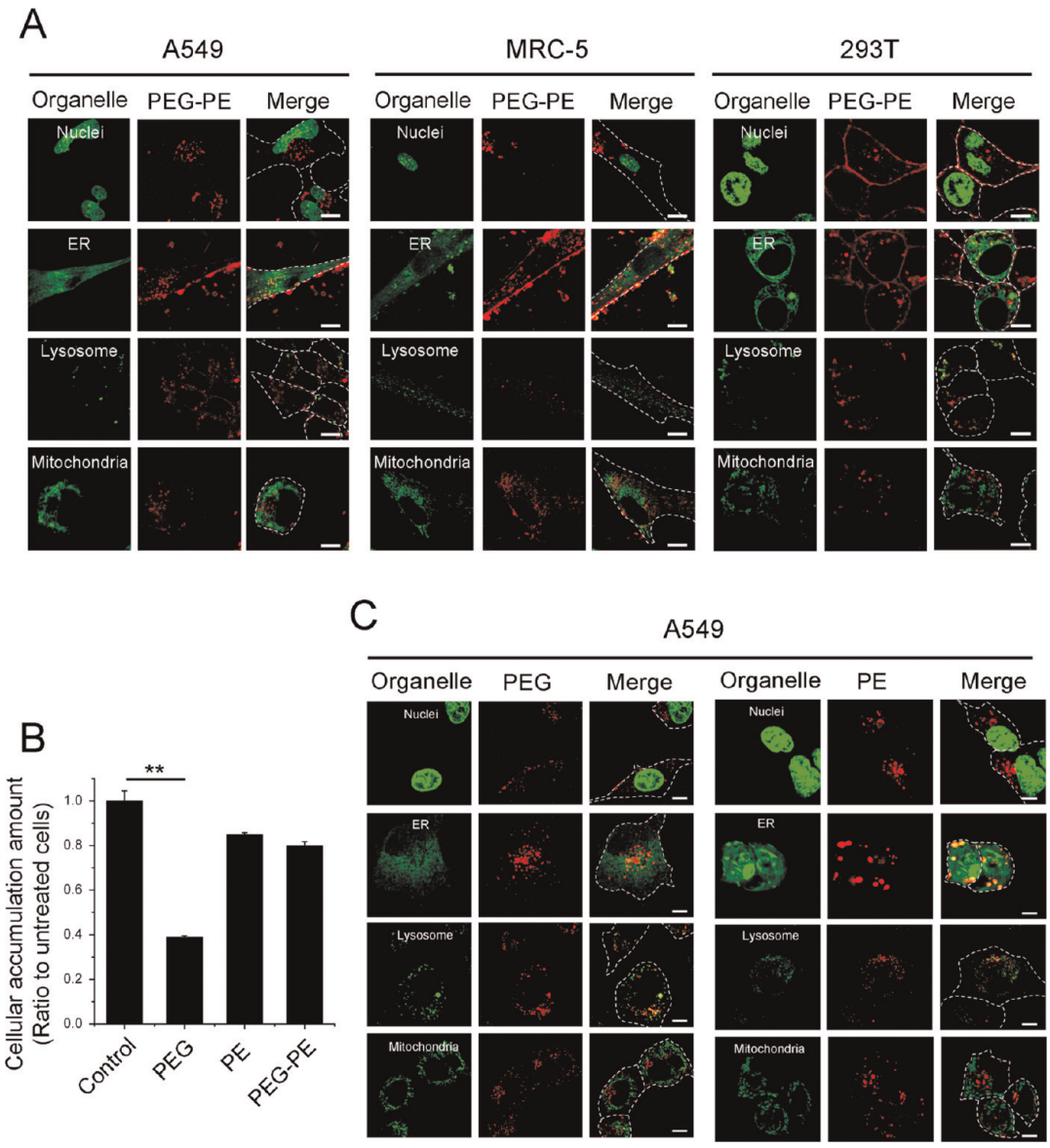

Figure 1. PEG–PE, similar to PE, accumulates in the ER. (A) Intracellular distribution of Alexa660-labeled PEG–PE in A549 cancer cells, MRC-5 cells, and 293T cells. (B) Macropinocytosis inhibitor wortmannin blocks the internalization of PEG, but not PE or PEG–PE. Cells were incubated with 100 nM wortamannin for 1 h and then with 70 μM fluorescent PEG, PE, or PEG–PE for 1 h. Cells not treated with the inhibitor were taken as controls. Cellular accumulation of fluorescent reagents was quantified by flow cytometry. (C) Intracellular distribution of Alexa660-labeled PEG and rhodamine B-labeled PE in A549 cancer cells. Organelle trackers are indicated in green, Alexa660-labeled PEG, rhodamine B-labeled PE and Alexa660-labeled PEG–PE are indicated in red, and their colocalization is indicated in yellow. Cell borders are delineated by white dashed lines. Scale bar = 5 μm. PEG: poly(ethylene glycol); PE: phosphoethanolamine.

and normal cells treated with PEG–PE micelles. Our experimental results strongly demonstrate that cancer cells undergo ER-dependent apoptosis in response to PEG–PE micelle treatment, while normal cells overcome the stress and survive. This ability of PEG–PE micelles to selectively induce cancer cell apoptosis without affecting normal cell function indicates that PEG–PE micelles are suitable carriers for delivery of anticancer drugs.

RESULTS

PEG–PE Micelles Induce ER Stress in Cancer Cells but not in Normal Cells. In a previous study, we showed that PEG–PE mainly accumulates in the ER in A549 cancer cells (derived from human lung carcinomas tissues).[10] In addition, we found that the intracellular distribution of Alexa660-labeled PEG–PE in MRC-5 cells (derived from normal human lung tissues) and 293T cells (derives from normal human kidney tissues) was similar to that in A549 cancer cells, indicating that the intracellular distribution of PEG–PE is independent of cell line (Figure 1A).

To further evaluate which of the blocks directs the ER accumulation of PEG–PE, we compared the internalization pathway and intracellular distribution of

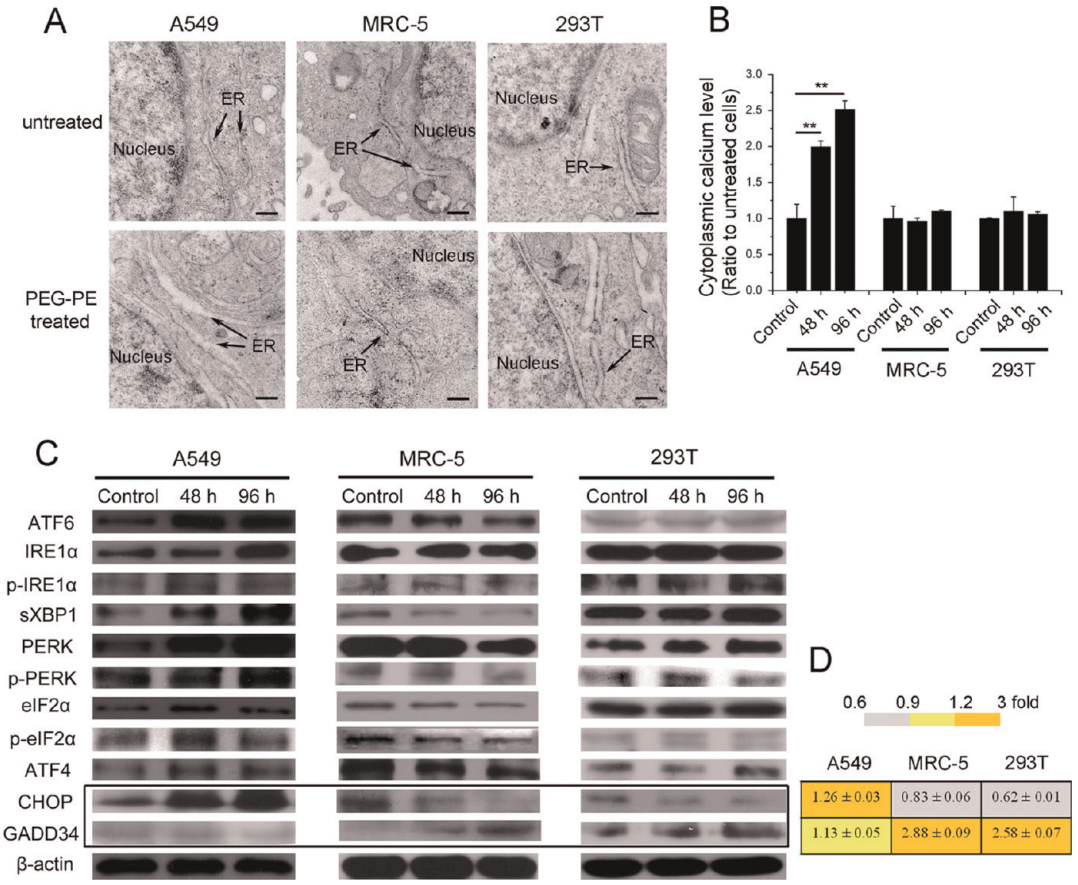

Figure 2. PEG–PE induces ER damage and UPR activation in A549 cancer cells but not in MRC-5 or 293T cells. (A) ER structures in PEG–PE-treated cells observed by TEM. Cells were incubated with 70 μM PEG–PE micelles for 48 h. Arrows indicate cisternae of the rough ER as delimited by electron-dense ribosomes. Scale bar = 200 nm. ER: endoplasmic reticulum. (B) Cytoplasmic calcium level and (C) expression of UPR-related proteins in PEG–PE-treated cells. Cells were incubated with 35 μM PEG–PE micelles for 48 or 96 h. (D) Relative mRNA levels of *chop* and *gadd34* in PEG–PE-treated cells. Cells were incubated with 35 μM PEG–PE micelles for 48 h. Untreated cells were taken as controls.

Alexa660-labeled PEG–PE, Alexa660-labeled PEG, and rhodamine B-labeled PE in A549 cancer cells. Since PEG binds many water molecules in aqueous medium[10] and PEG uptake was blocked by wortmannin (Figure 1B), an inhibitor which blocks macropinocytosis,[14] we concluded that PEG was taken up by cells through macropinocytosis. However, wortmannin did not affect the internalization of PE and PEG–PE. In addition to their similar internalization pathway, PEG–PE also had a similar intracellular distribution to PE. Like PEG–PE, PE mainly accumulated in the ER; however, PEG was largely trapped in lysosomes (Figure 1C). The ER accumulation of PE induces ER stress and affects cellular functions, as evidenced by increased levels of cytoplasmic calcium, activated UPR, decreased mitochondrial membrane potential and up-regulated lipid synthesis in A549 cancer cells which were incubated with 35 μM PE for 48 h (Figure S1).

To address whether the influence of PEG–PE on the ER is similar to that of PE, we examined ER morphology, ER membrane integrity, and the expression of UPR-related proteins in PEG–PE-treated A549 cancer cells, MRC-5 cells, and 293T cells. Direct observations of ER structures were made using transmission electron microscopy (TEM). As shown in Figure 2A, the ER structures in PEG–PE-treated MRC-5 and 293T cells did not change markedly, appearing as a normal membrane network of cisternae delimited by electron-dense ribosome dots in the perinuclear space. However, PEG–PE-treated A549 cancer cells displayed abnormal ER structures with dilations and clefts, similar to cells with palmitate-induced ER stress.[15] Accordingly, increased levels of cytoplasmic calcium in PEG–PE-treated A549 cancer cells demonstrated ER membrane damage and leakage of ER calcium to the cytoplasm (Figure 2B). The ER is the major intracellular calcium storage compartment and plays a critical role in maintenance of cellular calcium homeostasis. If the ER membrane is damaged under unresolved stress, calcium effuses from the ER to the cytoplasm, resulting in an increase in the fluorescence intensity of calcium-sensitive probe Fluo-4-AM.

Dilated ER structures and damaged ER membranes suggest that PEG–PE induces unresolved ER stress in A549 cancer cells (Figure 2A, 2B). ER stress initiates UPR activation *via* three ER sensors: ATF6, IRE1α, and PERK.[16] Cleaved ATF6 is transported to the nucleus

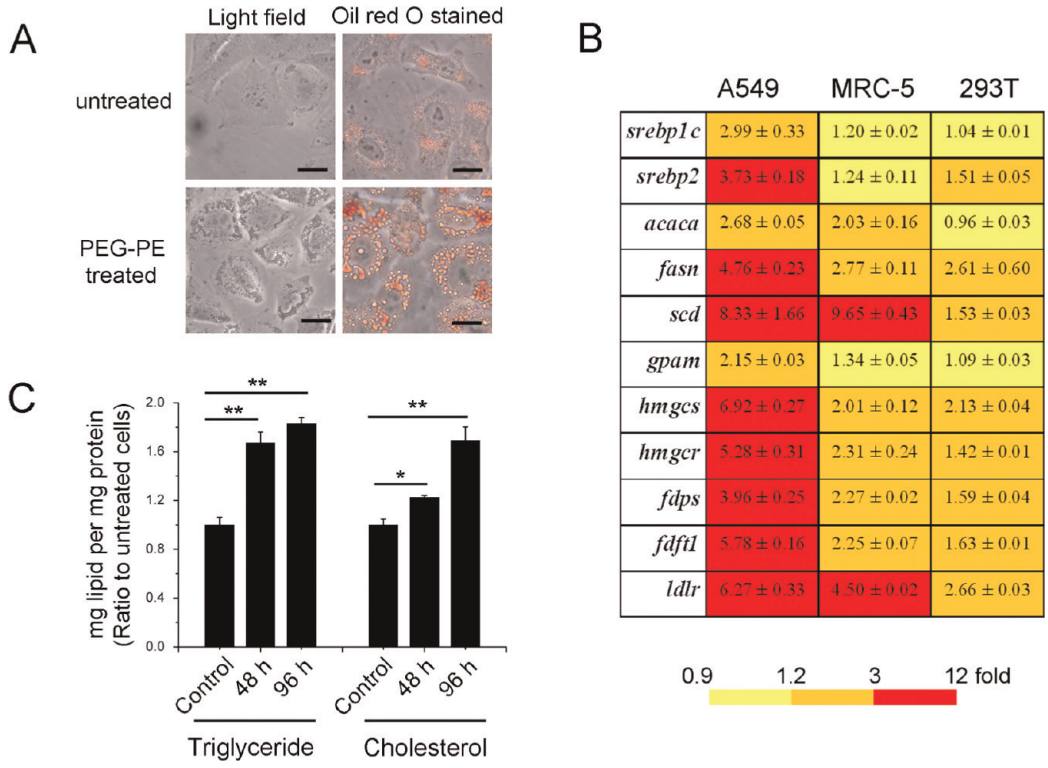

Figure 3. PEG–PE triggers lipid accumulation in A549 cancer cells. (A) Light microscope images of PEG–PE-treated A549 cancer cells. After incubation with 35 μM PEG–PE micelles for 5 d, cells were stained with oil red O. Scale bar = 10 μm. (B) Relative mRNA levels of lipid synthesis-related genes in PEG–PE-treated cells. Cells were incubated with 35 μM PEG–PE micelles for 48 h. Untreated cells were taken as controls: *srebp*, sterol regulatory element-binding protein; *acaca*, acetyl-CoA carboxylase; *fasn*: fatty acid synthase; *scd*, steatoyl-CoA desaturase; *gpam*, glycerol-3-phosphate acyltransferase; *hmgcs*, HMG-CoA synthase; *hmgcr*, HMG-CoA reductase; *fdps*, farnesyl diphosphate synthase; *fdft1*, farnesyl diphosphate farnesyltransferase 1; *ldlr*, low-density lipoprotein receptor. (C) Triglyceride and total cholesterol mass in PEG–PE-treated A549 cancer cells. Cells were incubated with 35 μM PEG–PE micelles for 48 or 96 h. Lipid mass was normalized by cellular protein mass.

upon ER stress and regulates UPR gene expression. Phosphor-IRE1α splices *xbp1* mRNA, and the encoded spliced XBP1 (sXBP1) protein is a transcriptional activator of UPR genes. Phosphor-PERK phosphorylates the α-subunit of eIF2α, phosphor-eIF2α activates ATF4, and ATF4 further up-regulates CHOP.[17] We measured the expression of UPR-related proteins in the three cell lines. As shown in Figure 2C, increased phosphorylation of IRE1α, PERK, and eIF2α correlated with increased expression of ATF6, sXBP1, ATF4, and CHOP, suggesting that all the three UPR signaling pathways were activated in PEG–PE-treated A549 cancer cells. In contrast, decreased or unchanged levels of UPR-related proteins in PEG–PE-treated MRC-5 and 293T cells indicated UPR negative feedback when cells overcame mild ER stress. During UPR activation, CHOP is the major promoter of ER stress-induced apoptosis, but GADD34 is involved in a negative feedback loop that down-regulates CHOP by dephosphorylating eIF2α.[18] Figure 2D and Figure 2C (circle) showed that the mRNA and protein levels of proapoptotic *chop* increased in PEG–PE-treated A549 cancer cells but decreased in MRC-5 and 293T cells. However, *gadd34* gave the opposite pattern of expression in the three cell lines compared to *chop*. When we alleviated ER stress with the UPR inhibitor 4-phenylbutyric acid (PBA), the level of cytoplamic calcium decreased to that of the controls, indicating that UPR activation induces ER membrane damage and ER calcium leakage (Figure 4C). Taken together, our data demonstrate that when PEG–PE accumulates in the ER, normal cells can overcome the stress and reach UPR feedback, but cancer cells cannot reestablish ER homeostasis and maintain a highly activated UPR, resulting in damage to ER structures and ER membrane integrity under unresolved stress. This implies that their different responses to PEG–PE accumulation in the ER may affect the cell fate of cancer cells and normal cells.

PEG–PE-Induced ER Stress Enhances Lipid Synthesis and Accumulation in A549 Cancer Cells. When A549 cancer cells were incubated with 35 μM PEG–PE micelles for up to 5 d, light microscope images showed that a lot of dark dots appeared in the cytoplasm, and oil red O staining demonstrated that these dots were lipid droplets (Figure 3A). Cellular lipid homeostasis is sensed and regulated by a family of membrane-bound transcription factors (SREBPs). SREBP1c preferentially enhances the transcription of genes required for fatty acid and triglyceride synthesis, while SREBP2 preferentially activates cholesterol synthesis and uptake.[19] As shown in

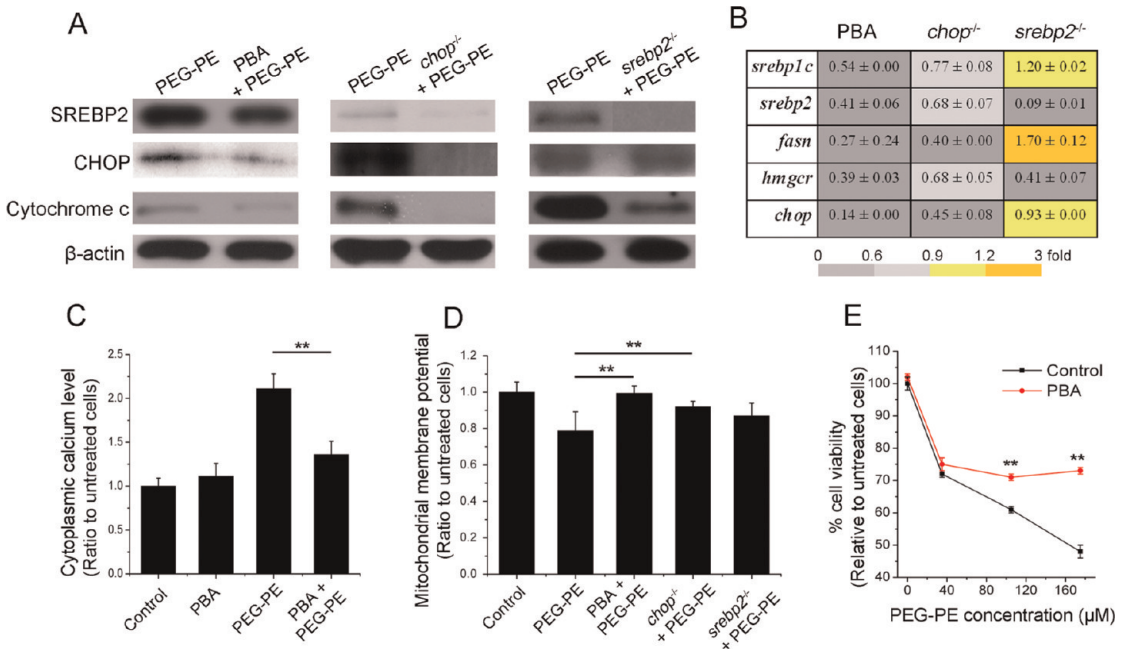

Figure 4. UPR inhibitor PBA and knockdown of *chop* alleviate PEG−PE-induced ER stress, lipid up-regulation, and apoptosis in A549 cancer cells. (A) Expression of SREBP2, CHOP, and cytochrome c protein, (B) relative mRNA levels of lipid synthesis-related genes, (C) cytoplasmic calcium level, and (D) mitochondrial membrane potential in PBA-pretreated A549 cancer cells, *chop*$^{-/-}$ A549 cancer cells and *srebp2*$^{-/-}$ A549 cancer cells. Cells were incubated with 35 μM PEG−PE micelles for 48 h. PEG−PE-treated mock-transfected cells were taken as controls. (E) PBA improves the viability of PEG−PE-treated A549 cancer cells. Cells were coincubated with 20 μM PBA and PEG−PE micelles for 48 h. PBA: 4-phenylbutyric acid.

Figure 3B, the relative mRNA levels of *srebp1c* and *srebp2* increased 2-fold and 2.7-fold, respectively, in PEG−PE-treated A549 cancer cells. SREBP1c-responsive genes include *acaca*, *fasn*, *scd*, and *gpam* which are involved in fatty acidy synthesis, and *gpam*, which encodes the first committed enzyme in triglyceride and phospholipid synthesis.[19] The relative mRNA levels of all these SREBP1c-responsive genes increased greatly in PEG−PE-treated A549 cancer cells. SREBP2 regulates cellular accumulation of cholesterol, including *de novo* cholesterol synthesis and the uptake of extracellular low-density lipoprotein (LDL) *via* the LDL receptor (LDLR) protein.[19] In PEG−PE-treated A549 cancer cells, the relative mRNA levels of cholesterol synthesis-related genes, including *hmgcs*, *hmgcr* (encoding the rate-limiting enzyme in cholesterol synthesis), *fdps*, *fdft1* ,and *ldlr*, all increased. Enhanced expression of SREBP1c- and SREBP2-responsive genes resulted in increased cellular accumulation of triglyceride and cholesterol in PEG−PE-treated A549 cancer cells (Figure 3C) which may be stored in lipid droplets (Figure 3A). Compared to A549 cancer cells, the relative mRNA levels of *srepb1c*, *srebp2*, and their related genes did not increase or only slightly increased in PEG−PE-treated MRC-5 and 293T cells (Figure 3B), and lipid droplets were not observed in the cytoplasm of these cells (data not shown).

Dysregulation of SREBP activation and cellular lipid accumulation are associated with ER stress and UPR, but it is unclear which occurs first. On the one hand, it has been reported that accumulation of cholesterol or fatty acids in the ER induces ER stress;[12,13] on the other hand, some studies have indicated that ER stress can activate SREBPs and induce lipid accumulation.[20] In order to clarify the relationship between lipid up-regulation and UPR activation in PEG−PE-treated A549 cancer cells, we attenuated these molecular events by chemical inhibitors and siRNA. PBA can inhibit UPR activation and relieves ER stress by stabilizing protein conformation, improving ER folding capacity and facilitating the trafficking of mutant proteins.[21] When A549 cancer cells were coincubated with 35 μM PEG−PE micelles and 20 μM PBA for 48 h, both the expression of CHOP protein and the level of cytoplasmic calcium decreased to that of the control (Figure 4A, 4C). In addition, the relative mRNA levels of lipid synthesis-related genes, including *srebp1c*, *srebp2*, *fasn*, and *hmgcr* and the expression of SREBP2 protein all decreased in PBA-treated A549 cancer cells (Figure 4A, 4B). Knockdown of *chop* also relieves ER stress and down-regulates UPR activation.[22] In *chop*$^{-/-}$ A549 cancer cells, the up-regulated lipid synthesis returned to almost baseline level (Figure 4B). In contrast, when cholesterol synthesis was inhibited by knocking down *srebp2*, the expression of CHOP did not change (Figure 4A). These data demonstrate that lipid production and accumulation results from PEG−PE-induced UPR activation in A549 cancer cells.

Cancer Cells and Normal Cells Have Different Cell Fates under PEG−PE-Induced ER Stress. Cells can survive under mild ER

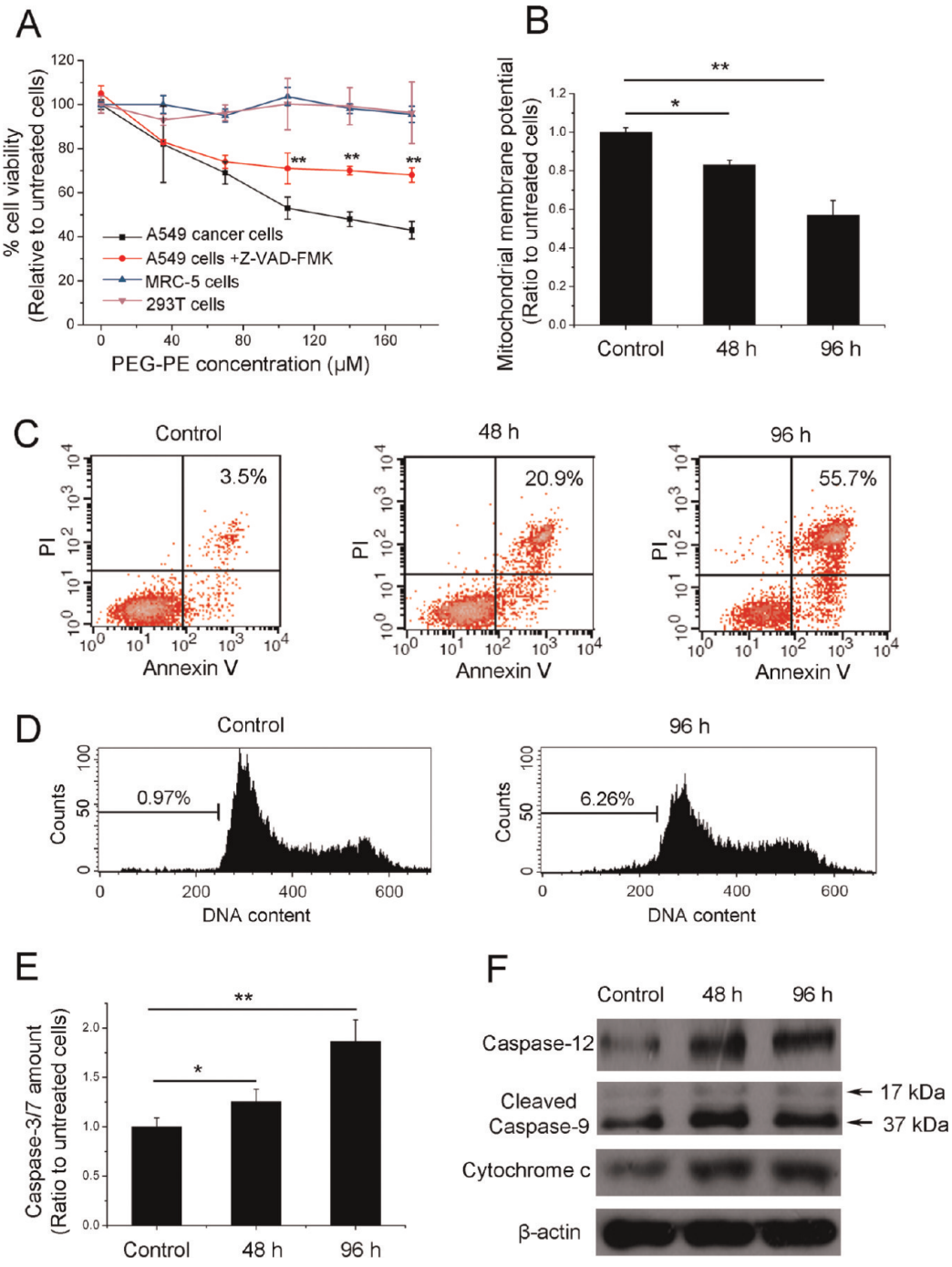

Figure 5. PEG–PE-induced ER stress triggers caspase-dependent apoptosis in A549 cancer cells: (A) PEG–PE induces cell death in A549 cancer cells but not in MRC-5 or 293T cells. The caspase inhibitor Z-VAD-FMK improves the viability of PEG–PE-treated A549 cancer cells. Cells were coincubated with 20 μM Z-VAD-FMK and PEG–PE micelles for 48 h. (B) Mitochondrial membrane potential, (C) Annexin V/PI analysis, (D) sub-G1 detection, (E) amount of caspase-3/7, (F) expression of caspase-12, cleaved caspase-9 and cytochrome c protein in PEG–PE-treated A549 cancer cells. Cells were incubated with 35 μM PEG–PE micelles for 48 or 96 h. In the Annexin V/PI analysis, the lower-right panel shows early apoptotic cells and the upper-right panel shows late apoptotic cells. PI: propidium iodide.

stress by initiating protective UPR signaling to restore homeostasis; under severe or prolonged ER stress, however, stress cannot be resolved, so UPR signaling switches to being proapoptotic and results in cell death.[23] The differences in UPR and the degree of ER damage between cancer cells and normal cells under PEG–PE-induced stress described above suggest that they might have different cell fates. To verify this, we incubated A549 cancer cells and MRC-5 and 293T cells with PEG–PE micelles for 48 h; A549 cancer cells died in a concentration-dependent manner, but the viability of MRC-5 and 293T cells was not affected (Figure 5A). Cell death can result from autophagy, necrosis, or apoptosis. Autophagy is marked by LC3B protein up-regulation and

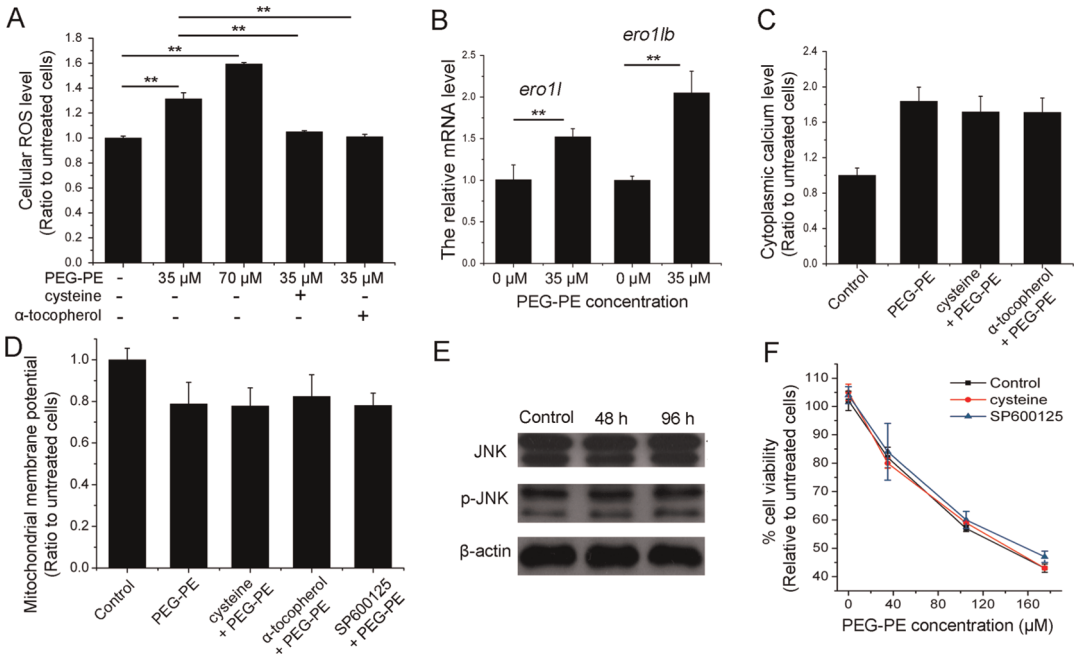

Figure 6. PEG–PE-induced apoptosis in A549 cancer cells is independent of oxidative stress and JNK. (A) Intracellular ROS levels increase in PEG–PE-treated A549 cancer cells. Reducing agents cysteine and α-tocopherol decrease PEG–PE-induced ROS production. ROS: reactive oxygen species. (B) Relative mRNA levels of *ero1l* and *ero1 lb* in PEG–PE-treated A549 cancer cells. Untreated cells were taken as controls. *ero*: endoplasmic reticulum oxidase. (C) Cytoplasmic calcium level and (D) mitochondrial membrane potential in A549 cancer cells coincubated with 35 μM PEG–PE micelles and 6 mM cysteine or 400 μM α-tocopherol or 20 μM SP600125 for 48 h. (E) Expression of JNK and phosphor-JNK (p-JNK) protein in A549 cancer cells. (F) Reducing agent cysteine and JNK inhibitor SP600125 do not improve the viability of PEG–PE-treated A549 cancer cells. Cells were coincubated with PEG–PE micelles and 6 mM cysteine or 20 μM SP600125 for 48 h. In (A), (B), and (E), cells were incubated with 35 μM PEG–PE micelles for 48 h.

autophagosome formation, and necrosis induces broken plasma membranes and leakage of cytosolic lactate dehydrogenase (LDH) at an early stage.[24] However, up-regulated LC3B protein and increased amounts of extracellular LDH were not observed in A549 cancer cells when cells were incubated with 35 or 70 μM PEG–PE micelles for 48 h (Figure S2, Supporting Information). Mitochondrial membrane potential decreased in PEG–PE-treated A549 cancer cells (Figure 5B). Annexin V/propidium iodide (PI) analysis showed that the proportions of both early apoptotic cells and late apoptotic cells increased with incubation time (Figure 5C). In addition, slight DNA damage was observed in A549 cancer cells after long incubations with PEG–PE micelles (Figure 5D). These data indicate that apoptosis occurs in PEG–PE-treated A549 cancer cells. As shown in Figure 5E,F, apoptosis in cancer cells is caspase-dependent; expression of caspase-3/7, caspase-12, cleaved caspase-9, and cytochrome c protein all increased after PEG–PE treatment in A549 cancer cells, and the general caspase inhibitor Z-VAD-FMK improved the viability of PEG–PE-treated cancer cells (Figure 5A). PEG–PE-induced ER stress, lipid up-regulation, and apoptosis were also observed in two other kinds of cancer cells, namely MCF-7 cancer cells (derived from human breast adenocarcinoma tissues) and 4T1 cancer cells (derived from mouse mammary gland tumor tissues) (Figure S3, Supporting Information). However, in PEG–PE-treated MRC-5 and 293T cells, LC3B up-regulation, LDH leakage, breakage of the mitochondrial membrane, and caspase-3/7 activation were not observed (Figure S2, Supporting Information), demonstrating that normal cells can successfully overcome PEG–PE-induced stress and survive. Though cancer cells did not have the same ability as normal cells to overcome PEG–PE-induced ER stress, they were able to relieve stress and decrease cell death under mild ER stress. When A549 cancer cells were treated with 35 μM PEG–PE micelles for 48 h and then incubated in micelle-free medium for another 48 h, levels of ER calcium were restored, mitochondrial membrane potential recovered, levels of cytochrome c were reduced and up-regulated lipid synthesis was alleviated (Figure S4, Supporting Information).

In addition to sustained ER stress, oxidative stress can also promote apoptosis.[2] Here, increased reactive oxygen species (ROS) were detected in PEG–PE-treated A549 cancer cells (Figure 6A), implying that PEG–PE-induced apoptosis may result from oxidative stress. To test the origin and role of ROS in relation to PEG–PE, we inhibited ER stress and oxidative stress, respectively, and detected changes in ER function, mitochondrial function, and cell fate. In the presence of reducing agents cysteine or α-tocopherol, cellular ROS levels decreased, but the PEG–PE-induced increased levels of cytoplasmic calcium, decreased mitochondrial membrane potential, and damaged cell

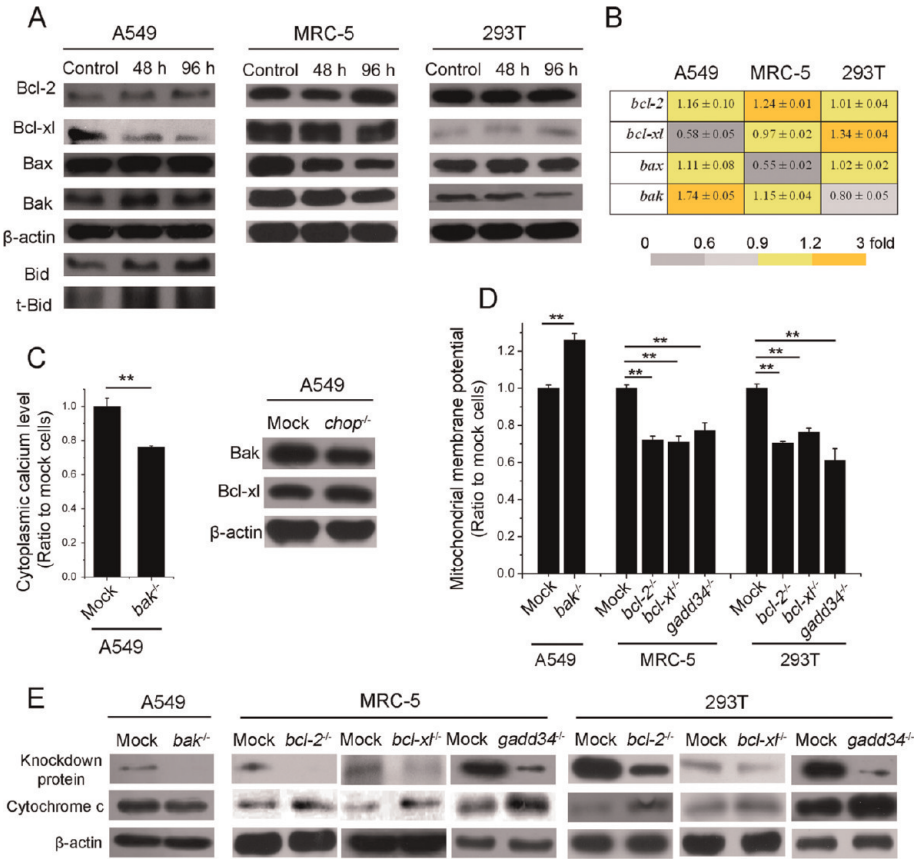

Figure 7. Bcl-2 family proteins, CHOP, and GADD34 determine cell fates under PEG–PE-induced ER stress. (A) Protein expression and (B) relative mRNA levels of Bcl-2 family genes in PEG–PE-treated cells. Cells were incubated with 35 μM PEG–PE micelles for 48 or 96 h. Untreated cells were taken as controls. (C) Knockdown of *bak* decreases cytoplasmic calcium level, while knockdown of *chop* down-regulates Bak but up-regulates Bcl-xl in PEG–PE-treated A549 cancer cells. (D, E) Knockdown of *bak* inhibits apoptosis in PEG–PE-treated A549 cancer cells, while knockdown of *bcl-2*, *bcl-xl* or *gadd34* induces apoptosis in PEG–PE-treated MRC-5 or 293T cells, indicated by changes of (D) mitochondrial membrane potential and (E) expression of cytochrome c. Mock-transfected cells and siRNA-transfected cells were incubated with 35 μM PEG–PE micelles for 48 h.

viability in PEG–PE-treated A549 cancer cells were not affected by these reducing agents (Figure 6C,D,F). In contrast, when ER stress was alleviated by the UPR inhibitor PBA or by knockdown of *chop*, apoptosis was inhibited, as evidenced by decreased levels of cytochrome c, recovery of mitochondrial membrane potential, and improved cell viability (Figure 4A,D,E). Taken together, we conclude that ER stress, but not oxidative stress, induces apoptosis in PEG–PE-treated A549 cancer cells. The increased relative mRNA levels of *ero1l* and *ero1 lb* imply that the increased ROS might be a byproduct of endoplasmic reticulum oxidase (ero) under PEG–PE-induced ER stress (Figure 6B).

Three pathways have been reported to play a role in ER stress-induced apoptosis, namely the proapoptotic pathway of CHOP, activation of caspase-12, and activation of JNK.[17,23] CHOP and caspase-12 were shown here to participate in PEG–PE-induced apoptosis (Figure 2C and Figure 5F). JNK and phosphor-JNK, however, showed no change in PEG–PE-treated A549 cancer cells, and the JNK inhibitor SP600125 did not improve cell viability (Figure 6E,F). These data suggest that PEG–PE-induced apoptosis is independent of JNK.

Bcl-2 Family Proteins and PERK-eIF2α-ATF4-CHOP-GADD34 Pathway Determine Cell Fate. Bcl-2 family proteins are important regulators of ER stress-induced apoptosis.[25] Overexpression of Bcl-2 or deficiency of Bax and Bak confer protection against lethal ER stress.[26] In PEG–PE-treated A549 cancer cells, antiapoptotic Bcl-xl decreased and proapoptotic Bak increased at both the mRNA and protein levels (Figure 7A,B). This result is in good agreement with a previous report that Bcl-xl, but not Bcl-2, targets Bak.[27] Enhanced expression of either Bax or Bak can cause their accumulation in the ER and mitochondria, and induce calcium leakage from the ER and cytochrome c release from mitochondria, finally leading to apoptosis.[28] After knocking down the *bak* gene in PEG–PE-treated A549 cancer cells, levels of ER calcium were restored, mitochondrial membrane was potential recovered, and levels of cytochrome c decreased (Figure 7C–E), demonstrating that Bax plays an important role in PEG–PE-induced apoptosis. Cytosolic Bid can be cleaved to tBid and then translocates to

mitochondria where it triggers the activation of Bak, inducing the release of cytochrome c.[29] Here, we also observed increased expression of Bid and truncated Bid (tBid) protein in PEG–PE-treated A549 cancer cells. In contrast to A549 cancer cells, increased levels of antiapoptotic Bcl-2 family proteins, including Bcl-2 and Bcl-xl, protected MRC-5 and 293T cells from PEG–PE-induced apoptosis. In PEG–PE-treated MRC-5 cells, Bcl-2 increased and Bax decreased, while in PEG–PE-treated 293T cells, Bcl-xl increased and Bak decreased (Figure 7A,B). Increased levels of cytoplamic calcium and decreased mitochondrial membrane potential were not observed in PEG–PE-treated MRC-5 and 293T cells (Figure 2B and Figure S2, Supporting Information), possibly because antiapoptotic Bcl-xl and Bcl-2 can antagonize the effects of proapoptotic Bax/Bak on the ER and mitochondrial permeability. After knocking down the *bcl-2* or *bcl-xl* gene, ER stress-induced apoptosis occurred in MRC-5 and 293T cells, as evidenced by decreased mitochondrial membrane potential and increased levels of cytochrome c (Figure 7D,E).

In addition to Bcl-2 family proteins, the PERK-eIF2α-ATF4-CHOP-GADD34 pathway in the UPR also plays a decisive role in cell fate determination under PEG–PE-induced ER stress. In PEG–PE-treated A549 cancer cells, phosphor-PERK phosphorylated eIF2α and further activated ATF4. ATF4 up-regulated CHOP, a direct and effective trigger of ER stress-induced apoptosis (Figure 2C and Figure 4).[30] When PEG–PE-induced ER stress and UPR activation were alleviated in A549 cancer cells by the UPR inhibitor PBA or by knocking down the *chop* gene, mitochondrial membrane potential recovered, levels of cytochrome c decreased, and cell viability improved (Figure 4A,D,E). In PEG–PE-treated MRC5 and 293T cells, high expression of GADD34 down-regulated CHOP by promoting the dephosphorylation of eIF2α in a negative feedback loop (Figure 2C). When we knocked down the *gadd34* gene in these normal cell lines, prosurvival signaling switched to proapoptotic signaling and resulted in decreased mitochondrial membrane potential and increased levels of cytochrome c (Figure 7D,E). Taken together, our results indicate that under PEG–PE-induced ER stress, the PERK-eIF2α-ATF4-CHOP-GADD34 pathway plays a proapoptotic role in A549 cancer cells by activating CHOP, but an antiapoptotic role in MRC-5 and 293T cells by activating GADD34 which then inhibits proapoptotic CHOP. CHOP and the Bcl-2 family proteins are closely related. CHOP can repress the expression of Bcl-2 family genes, increasing the proportion of proapoptotic Bcl-2 family proteins. It has been reported that overexpression of CHOP induces apoptosis, and is associated with the activation and mitochondrial translocation of Bax.[22] Similarly, in PEG–PE-treated *chop*$^{-/-}$ A549 cancer cells, Bak decreased and Bcl-xl increased (Figure 7C), demonstrating that CHOP interacts with Bcl-2 family proteins to coregulate ER stress-induced apoptosis.

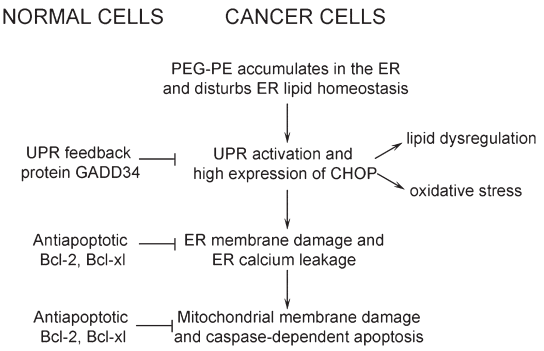

Scheme 1. Relationship between PEG–PE-Induced Molecular Events in Cancer Cells and Normal Cells

DISCUSSION

In this study, we found that PEG–PE selectively accumulates in the ER and induces ER stress. Proapoptotic and prosurvival UPR are triggered, respectively, in cancer cells and normal cells under this stress, leading to different cell fates (Scheme 1). PEG–PE-induced ER stress probably results from the disturbance of ER membrane lipid homeostasis owing to accumulation of PEG–PE in the ER. PEG–PE copolymers translocate to the ER *via* vesicle trafficking after being inserted into the cell membrane.[10] This specific ER distribution of PEG–PE, similar to PE, may disturb ER lipid homeostasis. Lipid homeostasis is important for ER functions, including protein-folding and lipid regulation.[11] Enrichment of the ER with cholesterol and inhibition of phosphatidylcholine synthesis have been reported to perturb the protein-folding environment and induce UPR activation.[31,32] Similarly, accumulation of PEG–PE or PE in the ER might also induce ER stress and activate UPR by changing ER lipid composition. UPR activation further triggers ER calcium leakage and apoptosis in PEG–PE-treated cancer cells. PEG–PE-induced UPR activation also increases lipid synthesis, possibly counteracting the PEG–PE-induced imbalance in lipid composition of the ER membranes; excess synthesized lipids are stored in lipid droplets in cancer cells. It has been reported that CdTe quantum dots can also trigger lipid droplet formation, but this lipid dysregulation is induced by oxidative stress.[33] In contrast to previous reports suggesting that ER stress and UPR activation can be induced by ER calcium depletion or oxidative stress,[34,35] we found that PEG–PE-induced UPR activation occurred prior to ER membrane damage and ROS production in A549 cancer cells, and that ROS plays a minor role in promoting apoptosis. Recent studies have demonstrated that the ER and mitochondria may interact with each other both spatially and functionally.[36] While increased mitochondrial superoxide in the electron transport chain during mitochondrial damage may cause ER stress, there is also

evidence showing that ER stress can induce mitochondria-related oxidative stress. ER stress can induce calcium leakage from the ER to the cytoplasm; the leaked calcium is taken up by mitochondria and causes disruption of the mitochondrial electron transport chain.[37]

The different ER responses and cell fates of cancer cells and normal cells under PEG–PE-induced ER stress can be explained by cell line-dependent differences in UPR and the expression of Bcl-2 family proteins. In contrast to normal cells, cancer cells require increased protein and lipid synthesis activities in the ER to accommodate their high proliferation rates, inducing physiological ER stress.[38] In addition, cancer cells are often exposed to hypoxia, nutrient starvation, oxidative stress, and other forms of metabolic dysregulation, which cause pathological ER stress.[39] Under both physiological and pathological ER stress conditions, cancer cells adapt and survive by initiating prosurvival UPR signaling. However, accumulation of PEG–PE in the ER disturbs ER lipid homeostasis, adding a further ER stress stimulus and leading to several important changes. First, small disturbances in the ER microenvironment may have a greater influence on the highly activated ER in cancer cells than on the strictly regulated ER in normal cells. In order to maintain active metabolism, cancer cells lack some feedback mechanisms for ER functions, such as the mechanism for inhibiting overactivated lipid synthesis.[40] When PEG–PE-induced ER stress activates SREBPs proteins and induces lipid synthesis, excess lipids are therefore stored in lipid droplets, adding a further burden to the cells. Second, chronic ER stress induced by PEG–PE micelles further increases the UPR activation of cancer cells. When cells are not able to resolve the cumulative stress, prosurvival UPR signaling switches to proapoptotic signaling and induce subsequent damage and cell death in cancer cells.[23] For these reasons, the accumulation of PEG–PE in the ER of cancer cells dilates the ER structure and triggers ER calcium release, which further induces mitochondrial dysfunction and finally apoptosis. During this process, Bcl-2 family proteins monitor incoming ER stress signals and also play a decisive role in determining cell fate.[25] Upon ER stress, proapoptotic Bax/Bak proteins translocate to the ER membrane and mediate a global increase in ER membrane permeability, resulting in ER calcium leakage and triggering downstream apoptosis signals.[41] This effect is antagonized by antiapoptotic Bcl-2 and Bcl-xl proteins. If antiapoptotic Bcl-2 family proteins are expressed at greater levels than proapoptotic Bcl-2 family proteins, cells will evade ER stress-induced damage and survive.[25] Because of differences in UPR signaling, cancer cells up-regulate proapoptotic Bax/Bak whereas normal cells up-regulate antiapoptotic Bcl-2 or Bcl-xl, leading to the different cell fates of cancer cells and normal cells under PEG–PE treatment.

Stress signals usually initiate from the organelle where the nanomaterial is located. Some nanomaterials enter the nucleus and cause genotoxic responses *via* direct interactions with DNA or DNA-related proteins. These interactions induce chromosomal fragmentation, DNA strand breakages, point mutations, oxidative DNA adducts, and alteration in gene expression profiles.[3] Some other nanomaterials directly lodge in mitochondria. This specific mitochondrial distribution probably disrupts mitochondrial electron transduction, leading to oxidative stress, or trafficking through the mitochondrial permeability transition pore, triggering the release of proapoptotic factors and programmed cell death.[2,4] If nanomaterials are targeted to the nucleus or mitochondria, serious cytotoxicity will be quickly induced. In the case of PEG–PE, PEG–PE copolymers preferentially accumulate in the ER and induce ER stress. Compared with genotoxicity and mitochondria-dependent toxicity, PEG–PE-induced ER stress is mild and resolvable, and results in differences in UPR signaling responses and cell fates between cancer cells and normal cells due to differences in their abilities to resolve ER stress. This not only demonstrates that PEG–PE can be used safely as a nanomaterial for drug delivery, but also implies that PEG–PE has the potential to enhance the anticancer effects of some chemotherapeutic drugs by selectively inducing ER stress and apoptosis in cancer cells.[42]

Comparison of the intracellular distribution and influence on cellular functions of PEG–PE with PE and PEG suggests that the cytotoxicity of copolymers probably largely depends on one of the blocks. If we can distinguish which of the copolymers is most cytotoxic, we can modify or substitute this block to minimize nanomaterial toxicity. PEG–PE has a similar intracellular distribution and cytotoxicity to the PE block. The nanomaterial used in this study was PEG2000-DSPE. When we substituted the saturated 1,2-distearoyl-*sn*-glycero-3-phosphoethanolamine (DSPE) block with unsaturated 1,2-dioleoyl-*sn*-glycero-3-phosphoethanolamine (DOPE), PEG–PE-induced ER damage and apoptosis in A549 cancer cells were alleviated; but when PEG2000 was changed to PEG5000, the effect of PEG–PE on cell viability was not markedly altered (Figure S5, Supporting Information).

In summary, our study demonstrates for the first time that PEG–PE can induce ER stress and that this stress results in different cell fates between cancer cells and normal cells. We further explain this difference by elaborating the decisive roles of UPR signaling pathways and Bcl-2 family proteins. Understanding the molecular mechanism underlying nanomaterial-induced cytotoxicity will help us better evaluate the safety and potential applications of various nanomaterials and will provide guidance for the design of new materials. We believe this study will provide a better

understanding of lipid-based nanomaterials and ER stress-related nanotoxicity.

CONCLUSION

PEG—PE copolymers accumulate in the ER and induce ER stress probably *via* disturbing ER lipid homeostasis. Under PEG—PE-induced ER stress, cancer cells initiate proapoptotic signaling while normal cells initiate prosurvival signaling, thus giving rise to different cell fates. In cancer cells, three UPR sensors, ATF6, IRE1α and PERK, and their downstream UPR-related proteins all increase under PEG—PE treatment. Highly activated UPR damages ER membranes, induces ER calcium release and further triggers caspase-dependent apoptosis by overexpression of CHOP, Bax/Bak. In addition, PEG—PE-induced UPR activation leads to lipid droplet formation and ROS production in cancer cells but not in normal cells. ER stress rather than oxidative stress is the main contributor to cancer cell apoptosis under PEG—PE treatment. In contrast, normal cells initiate prosurvival signaling in response to PEG—PE-induced ER stress, including increased expression of the UPR feedback protein GADD34, and antiapoptotic Bcl-xl or Bcl-2, and therefore, normal cells overcome the stress and survive.

MATERIALS AND METHODS

Materials. PEG2000-DSPE was purchased from Avanti Polar Lipids. SREBP2 antibody was kindly provided by Prof. Pingsheng Liu. The antibodies for PERK, phosphor-PERK, IRE1α, phosphor-IRE1α, CHOP, JNK, phosphor-JNK, cleaved caspase-9, and cytochrome c were purchased from Cell Signaling Technology. All other antibodies and all siRNAs were purchased from Santa Cruz. Hoechst 33342, Lysotracker Green, Mitotracker Green, Fluo-4-AM, $DiOC_6$, rhodamine B-labeled DSPE, and Lipofectamine2000 were purchased from Invitrogen. DsRed-ER plasmid was kindly provided by Prof. Tao Xu. All of the inhibitors and other chemical reagents were purchased from Sigma-Aldrich. Cell culture media and fetal bovine serum were purchased from Gibco. Alexa660-labeled PEG2000-DSPE and Alexa660-labeled PEG2000 were synthesized according to a previously published method.[10]

Cell Culture. A549 cancer cells (human nonsmall-cell lung cancer cells), MRC-5 cells (human fetal lung fibroblast cells), and 293T cells (human kidney epithelial cells containing Adeno and SV-40 DNA sequences) were purchased from the American Type Culture Collection (ATCC). Cells were cultured in RPMI 1640, MEM and DMEM, respectively, supplemented with 10% heat-inactivated fetal bovine serum, penicillin (100 U/mL), and streptomycin (100 U/mL).

Quantitative RT-PCR and siRNA Transfection. Total RNA was extracted from cells using a Purelink RNA mini kit (Invitrogen) and then reverse-transcribed into cDNA using oligo-dT and Superscript II. Relative mRNA levels of genes were measured with a SYBR Green qRT-PCR kit (Invitrogen) using a Rotor-gene 6200 (Corbett Life Science) with the following program: (i) 50 °C for 2 min, 1 cycle; (ii) 95 °C for 2 min, 1 cycle; (iii) 95 °C for 15 s and 60 °C for 30 s, 40 cycles. The *β-actin* mRNA level was used to normalize different loading amounts. Primer sequences are summarized in Supporting Table 1, (Supporting Information). siRNA or Ds-Red ER plasmid transfection was performed using Lipofectamine2000.

Oil Red O Staining and Lipid Quantification. After incubation with PEG—PE micelles for the times indicated, cells were first fixed with 10% formaldehyde for 30 min and then stained with oil red O solution for 30 min. Cells were photographed using a light microscope equipped with a camera (Nikon). To determine amount of cellular triglyceride and cholesterol, total cellular lipids were extracted with isopropanol and quantified using a triglyceride quantification kit and a total cholesterol assay kit (Invitrogen), respectively. The amount of cellular lipid was normalized using the amount of cellular protein.

ER Function, Mitochondrial Function, and Cell Viability Assays. Cytoplasmic calcium level was determined by Fluo-4-AM. Cells were first incubated with 5 μM Fluo-4-AM for 1 h at 37 °C, rinsed, and then incubated in phosphate-buffered saline (PBS) supplemented with 1% fetal bovine serum for another 1 h at 37 °C. Mitochondrial membrane potential was assessed by $DiOC_6$. The harvested cells were suspended in PBS with 40 nM $DiOC_6$ and incubated for 30 min at 4 °C. Cellular fluorescence intensity of Fluo-4-AM or $DiOC_6$ was quantified using a FACS Calibur flow cytometry (BD). Cell viability was assessed using the methylthiazoletetrazolium (MTT) method according to a previously published method.[9] The amount of lactate dehydrogenase (LDH) in the culture medium, the amount of cellular caspase-3/7, the level of cellular reactive oxygen species (ROS), Annexin V/PI analysis, and sub-G1 measurement were detected using commercial assay kits (Promega).

Organelle Staining. To visualize the ER, cells were transfected with a DsRed-ER plasmid and then incubated with 35 μM Alexa660-labeled PEG, rhodamine B-labeled PE, or Alexa660-labeled PEG—PE for 12 h. To visualize other organelles, cells were first incubated with fluorescent PEG, PE, or PEG—PE micelles for 12 h and rinsed, and then living cells were incubated with 10 μM Hoechst33342 for 30 min, 50 nM LysoTracker Green for 10 min, or 100 nM MitoTracker Green for 30 min to visualize the nucleus, lysosomes, and mitochondria, respectively. Co-localization of Alexa660-labeled PEG—PE, Alexa660-labeled PEG, or rhodamine B-labeled PE with different fluorescent organelle trackers was observed with a LSCMFV1000 confocal system (Olympus).

Transmission Electron Microscopy (TEM). Cells were incubated with 70 μM PEG—PE micelles for 48 h and then harvested, fixed with 2.5% glutaraldehyde in 0.1 M sodium cacodylate buffer for 24 h, and subsequently postfixed in 1% osmium tetroxide for 2 h. Specimens were dehydrated in a graded series of acetone and embedded in epoxy resin. After ultramicrotomy, ultrathin sections were stained with uranyl acetate for 15 min and modified with lead citrate for 5 min. Finally, subcellular structures were observed by TEM (Tecnai Spirit 120 kV, FEI).

Statistical Analysis. Results were presented as means ± SD unless noted otherwise. Differences in variables between groups were assessed using the student's *t*-test. *p* values less than 0.05 are indicated by *, and *p* values less than 0.01 are indicated by **. All experiments were performed at least three times.

Conflict of Interest: The authors declare no competing financial interest.

Acknowledgment. This work was supported by grants from the National Science and Technology Special Project of Major New Drugs Creation (2009ZX09501-025) and the National Nature Sciences Foundation of China (81173012). We thank Lei Sun for transmission electron microscopy and Zhenwei Yang for assistance with quantitative RT-PCR experiments.

Supporting Information Available: PE-induced ER stress and lipid up-regulation in A549 cancer cells (Figure S1); influence of PEG—PE micelles on viability of MRC-5 cells, 293T cells (Figure S2), 4T1 cancer cells, and MCF-7 cancer cells (Figure S3); recovery of A549 cancer cells from PEG—PE-induced ER stress (Figure S4); cytotoxicity of different kinds of PEG—PE micelles (Figure S5); and primers for different genes (Supporting Table 1). This material is available free of charge via the Internet at http://pubs.acs.org.

REFERENCES AND NOTES

1. Maynard, A. D.; Aitken, R. J.; Butz, T.; Colvin, V.; Donaldson, K.; Oberdorster, G.; Philbert, M. A.; Ryan, J.; Seaton, A.; Stone, V.; et al. Safe Handling of Nanotechnology. *Nature* **2006**, *444*, 267–269.

2. Nel, A.; Xia, T.; Madler, L.; Li, N. Toxic Potential of Materials at the Nanolevel. *Science* **2006**, *311*, 622–627.
3. Singh, N.; Manshian, B.; Jenkins, G. J.; Griffiths, S. M.; Williams, P. M.; Maffeis, T. G.; Wright, C. J.; Doak, S. H. Nanogenotoxicology: The DNA Damaging Potential of Engineered Nanomaterials. *Biomaterials* **2009**, *30*, 3891–3914.
4. Aillon, K. L.; Xie, Y.; El-Gendy, N.; Berkland, C. J.; Forrest, M. L. Effects of Nanomaterial Physicochemical Properties on *in vivo* Toxicity. *Adv. Drug Delivery Rev.* **2009**, *61*, 457–466.
5. Jain, K.; Kesharwani, P.; Gupta, U.; Jain, N. K. Dendrimer Toxicity: Let's Meet the Challenge. *Int. J. Pharm.* **2010**, *394*, 122–142.
6. Wang, X.; Kan, B.; Wang, Y.; Dong, P.; Shi, S.; Guo, G.; Zhao, Y.; Luo, F.; Zhao, X.; Wei, Y.; Qian, Z. Safety Evaluation of Amphiphilic Three-Armed Star-Shaped Copolymer Micelles. *J. Pharm. Sci.* **2010**, *99*, 2830–2838.
7. Lavasanifar, A.; Samuel, J.; Kwon, G. S. Poly(ethylene oxide)-*block*-Poly(L-amino acid) Micelles for Drug Delivery. *Adv. Drug Delivery Rev.* **2002**, *54*, 169–190.
8. Torchilin, V. P. Micellar Nanocarriers: Pharmaceutical Perspectives. *Pharm. Res.* **2007**, *24*, 1–16.
9. Tang, N.; Du, G.; Wang, N.; Liu, C.; Hang, H.; Liang, W. Improving Penetration in Tumors with Nanoassemblies of Phospholipids and Doxorubicin. *J. Natl. Cancer Inst.* **2007**, *99*, 1004–1015.
10. Wang, J.; Wang, Y.; Liang, W. Delivery of Drugs to Membreanes by Encapsulation in PEG−PE Micelles. *J. Controlled Release* **2012**, in press, doi: 10.1016/j.jconrel.2012.02.021.
11. Kim, I.; Xu, W.; Reed, J. C. Cell Death and Endoplasmic Reticulum Stress: Disease Relevance and Therapeutic Opportunities. *Nat. Rev. Drug Discovery* **2008**, *7*, 1013–1030.
12. Feng, B.; Yao, P. M.; Li, Y.; Devlin, C. M.; Zhang, D.; Harding, H. P.; Sweeney, M.; Rong, J. X.; Kuriakose, G.; Fisher, E. A.; et al. The Endoplasmic Reticulum is the Site of Cholesterol-Induced Cytotoxicity in Macrophages. *Nat. Cell Biol.* **2003**, *5*, 781–792.
13. Pineau, L.; Colas, J.; Dupont, S.; Beney, L.; Fleurat-Lessard, P.; Berjeaud, J. M.; Berges, T.; Ferreira, T. Lipid-Induced ER Stress: Synergistic Effects of Sterols and Saturated Fatty Acids. *Traffic* **2009**, *10*, 673–690.
14. Huth, U. S.; Schubert, R.; Peschka-Suss, R. Investigating the Uptake and Intracellular Fate of pH-Sensitive Liposomes by Flow Cytometry and Spectral Bio-Imaging. *J. Controlled Release* **2006**, *110*, 490–504.
15. Borradaile, N. M.; Han, X.; Harp, J. D.; Gale, S. E.; Ory, D. S.; Schaffer, J. E. Disruption of Endoplasmic Reticulum Structure and Integrity in Lipotoxic Cell Death. *J. Lipid Res.* **2006**, *47*, 2726–2737.
16. Ron, D.; Walter, P. Signal Integration in the Endoplasmic Reticulum Unfolded Protein Response. *Nat. Rev. Mol. Cell Biol.* **2007**, *8*, 519–529.
17. Szegezdi, E.; Logue, S. E.; Gorman, A. M.; Samali, A. Mediators of Endoplasmic Reticulum Stress-Induced Apoptosis. *EMBO Rep.* **2006**, *7*, 880–885.
18. Novoa, I.; Zeng, H.; Harding, H. P.; Ron, D. Feedback Inhibition of the Unfolded Protein Response by GADD34-Mediated Dephosphorylation of eIF2α. *J. Cell Biol.* **2001**, *153*, 1011–1021.
19. Horton, J. D.; Goldstein, J. L.; Brown, M. S. SREBPs: Activators of the Complete Program of Cholesterol and Fatty Acid Synthesis in the Liver. *J. Clin. Invest.* **2002**, *109*, 1125–1131.
20. Colgan, S. M.; Tang, D.; Werstuck, G. H.; Austin, R. C. Endoplasmic Reticulum Stress Causes the Activation of Sterol Regulatory Element Binding Protein-2. *Int. J. Biochem. Cell Biol.* **2007**, *39*, 1843–1851.
21. Welch, W. J.; Brown, C. R. Influence of Molecular and Chemical Chaperones on Protein Folding. *Cell Stress Chaperones* **1996**, *1*, 109–115.
22. McCullough, K. D.; Martindale, J. L.; Klotz, L. O.; Aw, T. Y.; Holbrook, N. J. Gadd153 Sensitizes Cells to Endoplasmic Reticulum Stress by Down-regulating Bcl2 and Perturbing the Cellular Redox State. *Mol. Cell. Biol.* **2001**, *21*, 1249–1259.
23. Boyce, M.; Yuan, J. Cellular Response to Endoplasmic Reticulum Stress: A Matter of Life or Death. *Cell Death Differ.* **2006**, *13*, 363–373.
24. Kepp, O.; Galluzzi, L.; Lipinski, M.; Yuan, J.; Kroemer, G. Cell Death Assays for Drug Discovery. *Nat. Rev. Drug Discovery* **2011**, *10*, 221–237.
25. Szegezdi, E.; Macdonald, D. C.; Ni-Chonghaile, T.; Gupta, S.; Samali, A. Bcl-2 Family on Guard at the ER. *Am. J. Physiol.: Cell Physiol.* **2009**, *296*, C941–953.
26. Wei, M. C.; Zong, W. X.; Cheng, E. H.; Lindsten, T.; Panoutsakopoulou, V.; Ross, A. J.; Roth, K. A.; MacGregor, G. R.; Thompson, C. B.; Korsmeyer, S. J. Proapoptotic BAX and BAK: A Requisite Gateway to Mitochondrial Dysfunction and Death. *Science* **2001**, *292*, 727–730.
27. Willis, S. N.; Chen, L.; Dewson, G.; Wei, A.; Naik, E.; Fletcher, J. I.; Adams, J. M.; Huang, D. C. Proapoptotic Bak Is Sequestered by Mcl-1 and Bcl-xL, but not Bcl-2, Until Displaced by BH3-Only Proteins. *Genes Dev.* **2005**, *19*, 1294–1305.
28. Nutt, L. K.; Pataer, A.; Pahler, J.; Fang, B.; Roth, J.; McConkey, D. J.; Swisher, S. G. Bax and Bak Promote Apoptosis by Modulating Endoplasmic Reticular and Mitochondrial Ca^{2+} Stores. *J. Biol. Chem.* **2002**, *277*, 9219–9225.
29. Wei, M. C.; Lindsten, T.; Mootha, V. K.; Weiler, S.; Gross, A.; Ashiya, M.; Thompson, C. B.; Korsmeyer, S. J. tBID, a Membrane-Targeted Death Ligand, Oligomerizes BAK to Release Cytochrome c. *Genes Dev.* **2000**, *14*, 2060–2071.
30. Zinszner, H.; Kuroda, M.; Wang, X.; Batchvarova, N.; Lightfoot, R. T.; Remotti, H.; Stevens, J. L.; Ron, D. CHOP Is Implicated in Programmed Cell Death in Response to Impaired Function of the Endoplasmic Reticulum. *Genes Dev.* **1998**, *12*, 982–995.
31. Li, Y.; Ge, M.; Ciani, L.; Kuriakose, G.; Westover, E. J.; Dura, M.; Covey, D. F.; Freed, J. H.; Maxfield, F. R.; Lytton, J.; Tabas, I. Enrichment of Endoplasmic Reticulum with Cholesterol Inhibits Sarcoplasmic-Endoplasmic Reticulum Calcium ATPase-2b Activity in Parallel with Increased Order of Membrane Lipids: Implications for Depletion of Endoplasmic Reticulum Calcium Stores and Apoptosis in Cholesterol-Loaded Macrophages. *J. Biol. Chem.* **2004**, *279*, 37030–37039.
32. van der Sanden, M. H.; Houweling, M.; van Golde, L. M.; Vaandrager, A. B. Inhibition of Phosphatidylcholine Synthesis Induces Expression of the Endoplasmic Reticulum Stress and Apoptosis-Related Protein CCAAT/Enhancer-Binding Protein-Homologous Protein (CHOP/GADD153). *Biochem. J.* **2003**, *369*, 643–650.
33. Przybytkowski, E.; Behrendt, M.; Dubois, D.; Maysinger, D. Nanoparticles Can Induce Changes in the Intracellular Metabolism of Lipids without Compromising Cellular Viability. *FEBS J.* **2009**, *276*, 6204–6217.
34. Cardozo, A. K.; Ortis, F.; Storling, J.; Feng, Y. M.; Rasschaert, J.; Tonnesen, M.; Van-Eylen, F.; Mandrup-Poulsen, T.; Herchuelz, A.; Eizirik, D. L. Cytokines Downregulate the Sarcoendoplasmic Reticulum Pump Ca^{2+} ATPase 2b and Deplete Endoplasmic Reticulum Ca^{2+}, Leading to Induction of Endoplasmic Reticulum Stress in Pancreatic Beta-Cells. *Diabetes* **2005**, *54*, 452–461.
35. Jeanson, L.; Kelly, M.; Coste, A.; Guerrera, I. C.; Fritsch, J.; Nguyen-Khoa, T.; Baudouin-Legros, M.; Papon, J. F.; Zadigue, P.; Prulière-Escabasse, V.; et al. Oxidative Stress Induces Unfolding Protein Response and Inflammation in Nasal Polyposis. *Allergy* **2012**, *67*, 403–412.
36. Pizzo, P.; Pozzan, T. Mitochondria-Endoplasmic Reticulum Choreography: Structure and Signaling Dynamics. *Trends Cell Biol.* **2007**, *17*, 511–517.
37. Görlach, A.; Klappa, P.; Kietzmann, T. The Endoplasmic Reticulum: Folding, Calcium Homeostasis, Signaling, and Redox Control. *Antioxid. Redox Signaling* **2006**, *8*, 1391–1418.
38. Wang, G.; Yang, Z. Q.; Zhang, K. Endoplasmic Reticulum Stress Response in Cancer: Molecular Mechanism and Therapeutic Potential. *Am. J. Transl. Res.* **2010**, *2*, 65–74.

39. Koumenis, C. ER Stress, Hypoxia Tolerance and Tumor Progression. *Curr. Mol. Med.* **2006**, *6*, 55–69.
40. Flavin, R.; Zadra, G.; Loda, M. Metabolic Alterations and Targeted Therapies in Prostate Cancer. *J. Pathol.* **2011**, *223*, 283–294.
41. Zong, W. X.; Li, C.; Hatzivassiliou, G.; Lindsten, T.; Yu, Q. C.; Yuan, J.; Thompson, C. B. Bax and Bak Can Localize To the Endoplasmic Reticulum to Initiate Apoptosis. *J. Cell Biol.* **2003**, *162*, 59–69.
42. Healy, S. J.; Gorman, A. M.; Mousavi-Shafaei, P.; Gupta, S.; Samali, A. Targeting the Endoplasmic Reticulum-Stress Response as An Anticancer Strategy. *Eur. J. Pharmacol.* **2009**, *625*, 234–246.